

# Research Journal of Pharmaceutical, Biological and Chemical Sciences

## Corrosion Protection Aspects of Mechanochemically Synthesized Polyaniline / MMT Clay Nanocomposites.

N Kalaivasan\*

Department of Chemistry, Thanthai Periyar Government Institute of Technology, Vellore - 632002, Tamil Nadu, India.

### ABSTRACT

Polyaniline (PANI)/ montmorillonite (MMT) nanocomposites were prepared by direct intercalation of anilinium ion into MMT galleries, followed by in-situ polymerization within the nano - interlamellar spaces under solvent- free mechanochemically method. After polymerization, X-ray diffraction and Fourier transform infrared analysis confirmed the successful synthesis of PANI chains between the MMT nanolayers. The surface morphologies of PANI-MMTs were strongly affected by the PANI content, were shown in the scanning electron microscopy (SEM) images. The synthesized polyaniline clay nanocomposites were treated with 0.1M HCl to get HCl doped PANI clay nanocomposites. PANI clay nanocomposites in the form of coatings on C45 steel were found much superior in corrosion protection over those of conventional polyaniline.

**Keywords:** Polyaniline, mechanochemical intercalation, nanocomposites, montmorillonite (MMT) clay, corrosion protection

*\*Corresponding author*

## INTRODUCTION

The use of conducting polymer for the protection of active metals against corrosion has received focused-attention in recent years [1-5]. In the past decade, use of polyaniline as anticorrosion coatings has been explored as the potential candidates to replace the chromium-containing materials, which have adverse health and environmental concerns [6-11]. Mangoli et al [12] was the first to examine the protective behavior of polyaniline on stainless steel and then in 1985, DeBerry [13] showed that the electrochemically synthesized polyaniline acts as corrosion protective layer on stainless steel in 1M H<sub>2</sub>SO<sub>4</sub>. Several research groups have systematically investigated the electrochemical synthesis of various conducting polymer on oxidizable metals for corrosion protection purpose [14-17]. Among the conducting polymers, polyaniline and polypyrrole are the most promising conducting polymers for corrosion protection of metals. The extent of using these conducting polymers is limited due to the exclusivity of the monomers that are essential for their synthesis [18]. To overcome this limitation, different synthesis approaches have been attempted. Recently, there are number of reports on the preparation and properties for the lamellar nanocomposites of polyaniline with various layered materials. In this paper, we present the first evaluation of corrosion protection effect for the mechanochemically synthesized HCl doped polyaniline clay nanocomposites on C45 steel. The corrosion studies such as polarization measurements and corrosion current were performed in 3.5 % NaCl electrolyte.

## EXPERIMENTAL METHODS

### Materials

The monomer aniline was purchased from Lancaster, UK. The N- methyl -2- pyrrolidone (NMP), N-N-dimethyl formamide (DMF), chloroform (CHCl<sub>3</sub>), hydrochloric acid (HCl) and ammonium persulphate ((NH<sub>4</sub>)<sub>2</sub> S<sub>2</sub>O<sub>8</sub>) were purchased from SD fine, India. Montmorillonite clay was obtained from Aldrich, USA.

### Characterization and Measurements

FT- IR spectra were recorded by Perkin- Elmer spectrometer (FT-IR, 16PC) using KBr pallets. All the spectra were recorded against the background spectrum of KBr. SEM studies were observed by FEI Quanta 200 Environmental Scanning Electron Microscope (ESEM) with EDAX EDS system. It was used to study the morphology of the various polymer clay nanocomposites. X-ray diffraction technique was used to study the amount of intercalation taking place between polymer and clay. XRD studies were recorded by BRUCKER, Germany make, Model:D8Advance, Source: 2.2 KW Cu anode, ceramic X- ray tube of lynx eye detector and zero background and PMMA sample holder was used.

### Corrosion studies

In corrosion studies, a working electrode was made of mild steel (C45). Chemical composition of C45 steel was (Wt. %): C = 0.46, Si = 0.40, Mn = 0.65, Cr = 0.40, MO = 0.10, Ni = 0.40 and other constituents = 0.63. It was manufactured as cylinder of 10mm height in a way to function as disk electrode with exposed area of 1.13 cm<sup>3</sup>, surrounded with Teflon tape. Before using, steel electrode was first polished on sand paper of 1000 grade then on a polishing cloth with alumina slurry (13µm). For drop coating of HCl doped PANI-MMT on steel electrode the PANI-MMT nanocomposites are dissolved in CHCl<sub>3</sub>. The steel electrode was previously polished with fine emery paper (p1000) and with alumina slurry (13µm).

### Polarization measurements

Anodic polarization measurements were carried out under ambient conditions in a three electrode single compartment cell containing 3.5% NaCl. C45 steel electrode (coated and uncoated) and a saturated calomel electrodes were used as a working electrode, reference electrode and counter electrode respectively, using a Solarton S11287 potentiostat connected to a computer via IEE 488.2 connections. Measurements were carried out at a scan rate of 5mV/s.

### Preparation of Sodium MMT

The montmorillonite 6 g was dispersed in 400mL aqueous acetone solution (1:1 by volume) and then treated with 600mL aqueous sodium chloride (10mM) at 50°C for 24 hours according to the literature method to yield sodium treated montmorillonite (Na-MMT) to extinguish the effect of other cations [19,20]. After repeated washing by filtration, the clay was dried at 80°C for 24 hours, ground to a fine powder, dried again at 120°C for further 24 hours, and stored in a desiccator.

### Preparation of PANI/MMT clay nanocomposites by mechanochemical method

The synthesis of the PANI and substituted PANI-MMT clay nanocomposites was carried out by mechanochemical intercalation method. The synthetic procedure for preparing PANI clay nanocomposites was as follows. The mixture of sodium MMT and anilinium chloride were mechanochemically ground with a mortar and pestle at room temperature with few drops of double distilled water for 10 minutes. The amount of added anilinium chloride was 4.6 mMol/g of MMT. After grinding, a sufficient amount of  $((\text{NH}_4)_2\text{S}_2\text{O}_8)$  was added, the molar ratio of  $((\text{NH}_4)_2\text{S}_2\text{O}_8)$  to anilinium chloride was 1.5. The mixture was added to the mortar and ground mechanochemically for 30 minutes [21]. The polymerization lasted for 72 hours at room temperature. After standing for 72 hours, the obtained dark green powder was washed with double distilled water and repeatedly filtering the solution in Buchner funnel in order to remove the excess  $((\text{NH}_4)_2\text{S}_2\text{O}_8)$ , by-products and sodium chloride produced by the cation of MMT and the anilinium cations of anilinium chloride. The washing was continuing until the filtrate become colourless. The final product was washed with methanol, distilled water and followed by dilute HCl. The HCl doped lamellar polymer clay nanocomposites were obtained. The product was drying under vacuum at room temperature for 12 hours and stored in a desiccator. The loading of anilinium ion varied from 1.25 and 4.6 mMol/ 1g of MMT.

## RESULT AND DISCUSSIONS

FT-IR Spectra of synthesized PANI-MMT nanocomposites together with those of pristine MMT and pure PANI prepared by conventional chemical oxidative polymerization is presented in Fig.1. Presence of conductive form of PANI in the clay was confirmed by FT-IR studies. The bands at 1600 and 1560  $\text{cm}^{-1}$  consist of benzenoid and quinoid form of polyaniline backbone and also these bands implies that the charge neutralization with the counter ion present in the polyaniline chain. The peaks at 1305 and 1245  $\text{cm}^{-1}$  are associated with the C-N stretching mode. The strong peak at 1041 $\text{cm}^{-1}$  and the peaks at 912 and 840  $\text{cm}^{-1}$  are the characteristic vibrations of MMT clay. In the higher frequency side a peak at 3250  $\text{cm}^{-1}$  is assigned for the N-H stretching vibrations (Fig.1).

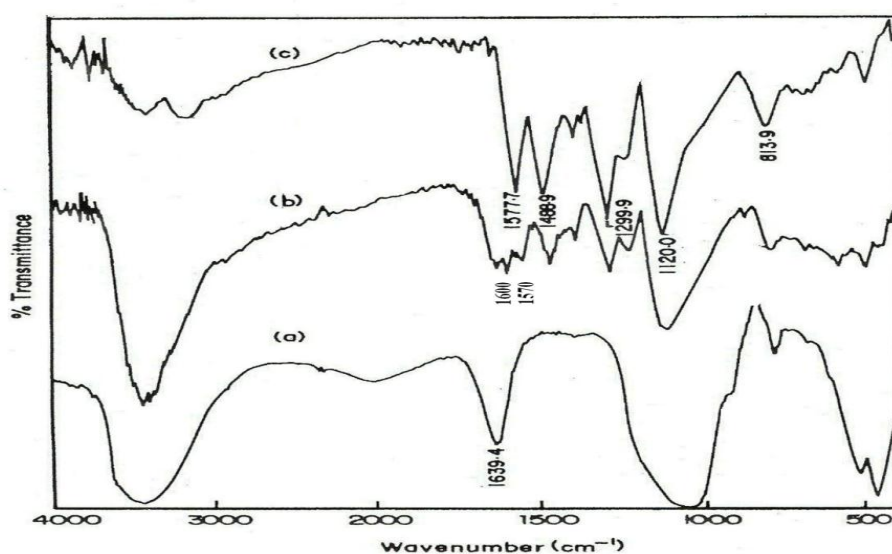


Figure 1: FT-IR spectrum of pristine clay (a), polyaniline clay nanocomposites (b) and chemically synthesized polyaniline (c)

The XRD patterns of the products by grinding aniline molecules with MMT in a mortar are shown in Fig.2. The red coloured powders of anilinium ion intercalated MMT clay compounds changed to dark green colour after polymerization. The products after polymerization of anilinium cation are denoted as polyaniline at different mMol of monomer / 1 g of MMT. Fig. 2, shows the XRD patterns of polyaniline obtained at 1.25 mMol of anilinium ion/ 1g of MMT and 4.6 mMol of anilinium ion/ 1g of MMT. After polymerization the basal spacing decreased from 1.48 to 1.25 nm for polyaniline obtained at 1.25mMol of anilinium ion/ 1g of MMT and from 2.47 to 1.33 nm for polyaniline obtained at 4.6 mMol of anilinium ion/ 1g of MMT.

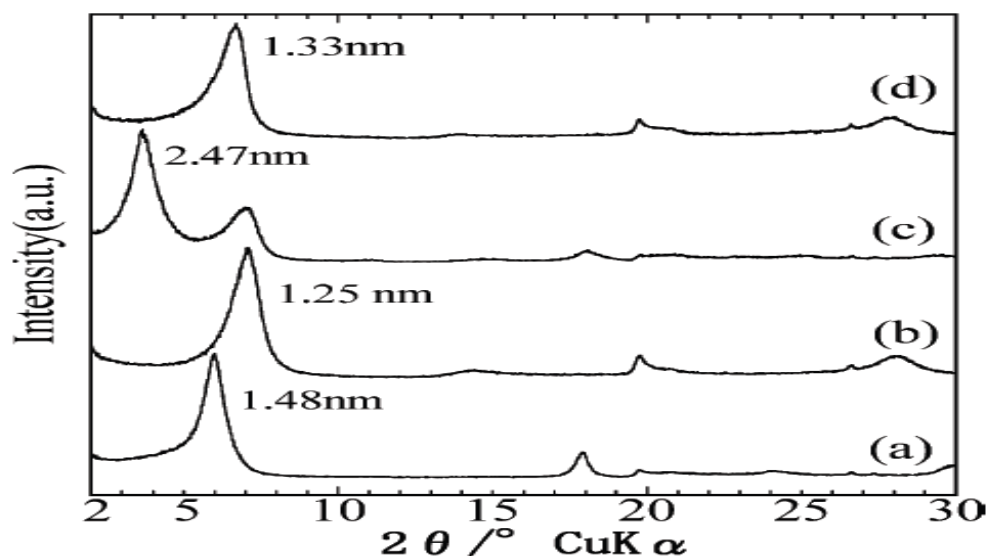
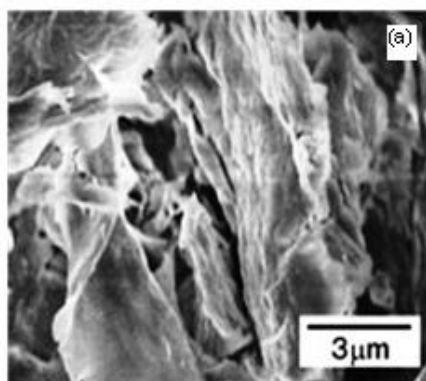


Figure 2: XRD patterns of anilinium cation at 1.25 mMol/ 1g of MMT (a), polyaniline clay nanocomposites at 1.25 mMol/ 1g of MMT (b), anilinium cation at 4.6 mMol/ 1g of MMT (c) and polyaniline clay nanocomposites at 4.6mMol/ 1g of MMT (d).

The XRD pattern shows the interlayer spacing after polymerization is less than those before polymerization for both samples [22]. These results would be expected to be in agreement with the observation that PANI forms a single chain with the extended chain conformation in the clay galleries as Wu *et al.* reported [23]. The slight differences in the interlayer spacing for both samples may be attributed to the amount of the intercalated species in the clay layers. That is, the larger amount of PANI would be synthesized in the clay layers for polyaniline obtained from 4.6 mMol of anilinium ion per 1 g of MMT, so that the basal spacing of this product was slightly greater than that of PANI obtained from 1.25 mMol of monomer per 1g of MMT. Hence for corrosion studies polyaniline obtained from the feed ratio 4.6mMol/ 1g of MMT was taken. The SEM micrograph of PANI-MMT nanocomposites with different PANI content, together with pristine MMT clay was shown in Fig.3. The SEM image shows that the surface morphologies of PANI-MMT nanocomposites are strongly affected by the PANI content in the nanocomposites.



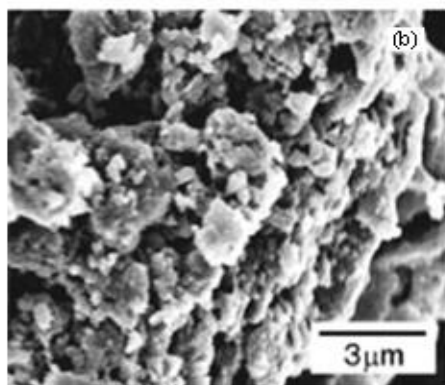


Figure 3: SEM images of pristine MMT clay (a), PANI clay nanocomposites by 4.6 mMol/gram of MMT (b).

The corrosion potential ( $E_{corr}$ ) and corrosion current density ( $i_{corr}$ ) can be obtained by polarization measurements. The equilibrium open circuit potential (OCP) of an electrode can be considered as  $E_{corr}$ . Corresponding to  $E_{corr}$  is  $i_{corr}$  which is proportional to corrosion rate ( $C_R$ ) as shown in the Eq.1 and has inverse relation with polarization resistance ( $R_p$ ) of electrode as shown in Eq.2 (rearrangement of Stern-Geary equation). The values of  $E_{corr}$ ,  $i_{corr}$  and Tafel slopes (anodic slope  $b_a$  and cathodic slope  $b_c$ ) can be obtained by extrapolation from Tafel plots. Using Eq.1 and Eq.2, the value of  $R_p$  and  $C_R$  of electrode can be easily determined.

$$i_{corr} = \frac{C_R \cdot A \cdot d}{0.129 \cdot (EW)} \quad (1)$$

Where  $i_{corr}$  is corrosion current density measured in  $\mu A \text{ cm}^{-2}$ ,  $C_R$  is corrosion rate measured in milliinch per year (MPY),  $d$  is density of material measured in  $\text{g cm}^{-3}$ ;  $EW$  is equivalent weight of corroded metal measured in g equivalent $^{-1}$ .

$$i_{corr} = \frac{b_a \cdot b_c}{2.303(b_a + b_c)} \cdot \frac{1}{R_p \cdot A} \quad (2)$$

Where  $i_{corr}$  is corrosion current density measured in  $\text{mA cm}^{-2}$ ,  $b_a$ ,  $b_c$  are anodic and cathodic Tafel slopes measured in  $\text{mV decade}^{-1}$ ,  $R_p$  is polarization resistance measured in ohm. Fig.4, shows Tafel plots of bare, passivated and PANI-MMT coated C45 steel electrodes. The values of  $E_{corr}$ ,  $i_{corr}$ ,  $b_a$ ,  $R_p$  and  $C_R$  of bare, passivated and PANI-MMT coated C45 steel electrodes are calculated and shown in Table 1. For passivated C45 steel,  $E_{corr}$  is negatively shifted by 15 mV compared to the bare C45 steel [24,25]. This shift showed cathodic protection of passive layer [26,27]. However,  $C_R$  did not decrease significantly. The corrosion potential of PANI-MMT coated C45 steel electrode is positively shifted by 51 mV compared to the bare C45 steel electrode. The shift of corrosion potential indicated that HCl doped PANI-MMT coating depressed the anodic current of the corrosion reaction. The increase of corrosion potential is an indication of anodic protection by doped PANI-MMT. As shown in the Table 1, the corrosion rate was significantly reduced for doped PANI-MMT coated C45 steel as compared to the bare C45 steel electrode.

Coating	$E_{corr, SCE}$ (mV)	$b_a$ (mV dec $^{-1}$ )	$i_{corr}$ ( $\mu A \text{ cm}^{-2}$ )	$R_p$ ( $\Omega$ )	$C_R$ (MPY)
Uncoated	-571	40.0	98.80	92	40.12
Passivated	-586	39.2	95.50	110	38.80
PANI-MMT	-520	35.5	19.90	519	8.10

Table 1:  $E_{corr}$ ,  $b_a$ ,  $i_{corr}$ ,  $R_p$  and  $C_R$  values calculated from Tafel plots for bare, passivated and PANI-MMT coated C45 steel electrode in 3.5 % NaCl.

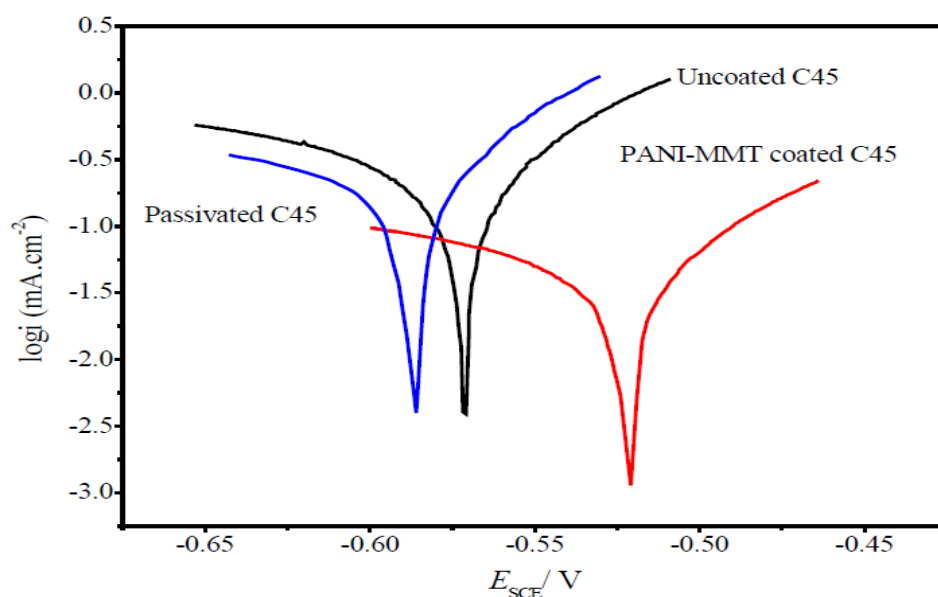


Figure 4: Tafel plot of uncoated, passivated and PANI-MMT coated C45 steel electrode in 3.5 % NaCl solution.

The polarization resistance  $R_p$  calculated from polarization measurements is in good agreement with  $R_{CT}$  value calculated from impedance measurements. The agreement between polarization resistance  $R_p$  (i.e. the slope of the current density versus electrode potential curve) and the sum of all Ohmic components in the electrode impedance deduced from impedance measurements at the same electrode potential is expected, because at frequency zero the sum of all Ohmic components of impedance is equal to said slope. The relatively small contribution of the film resistance  $R_f$  and solution resistance  $R_s$  results in a fairly good agreement between the  $R_p$  and  $R_{CT}$  in the present study.

### CONCLUSIONS

The polyaniline clay nanocomposites were successfully coated on C45 steel on drop coating and the corrosion protective aspects of these coatings in aqueous 3.5 NaCl solutions was investigated by polarization measurements. The result shows the corrosion rate was significantly reduced for doped PANI-MMT nanocomposites coated C45 steel as compare to the bare C45 steel. The FT-IR spectral studies and XRD patterns confirms the presence of conductive form of PANI chains in the MMT clay nanolayers. SEM micrograph shows that the surface morphologies of PANI/MMT nanocomposites are strongly affected by the amount of PANI content in the MMT clay.

### ACKNOWLEDGEMENT

The author gratefully acknowledges the School of Advanced Sciences, VIT University, Vellore, India and the Department of Chemistry, Thanthai Periyar Government Institute of Technology, Vellore, India for their assistance to bring out this paper in a reputed journal.

### REFERENCES

- [1] DE Tallman, G Spinks, A Dominis and G Wallace. J Solid State Electrochem 2002;6:73 - 84.
- [2] G Spinks, A Dominis, G Wallace and DE Tallman. J Solid State Electrochem 2002;6:85 - 100.
- [3] MC Bernard, S Joiret, AH Le-Goff and PD Long. J Electrochem Soc 2001;148:B299 - B303.
- [4] JI Martins, TC Reis, M Bazzouai, EA Bazzouai and LI Martins. Corros Sci 2004;46:2361 - 2381.
- [5] NA Ogurtsov, AA Pud, P Kamarchik and GS Shapoval. Synth Met 2004;143(1):43 - 47.



- [6] DW Deberry. *J Electrochem Soc* 1985;132:1027 - 1032.
- [7] B Wessling. *Synth Met* 1991;907:1057 - 1062.
- [8] JM Yeh, SJ Liou, CY Lai, PC Wu and JY Tsai. *Chem Mater* 2001;13(3):1131-1136.
- [9] DA Wroblewski, BC Benicewicz, KG Thompson and CJ Bryan. *Am Chem Soc Div Polym Chem* 1994;35(1):265 - 266.
- [10] B Wessling. *Adv Mater* 1994;6:226 - 228.
- [11] Y Wei, J Wang, X Jia, JM Yeh and P Spellance. *Polymer* 1995;36:4535 – 4537.
- [12] G Mongoli, M Munari, P Bianco and S Misiani. *J Appl Polym Sci* 1981;26:427- 432.
- [13] MH Al-Saleh, and U Sundararaj. *Polymer* 2010;51:2740-2747.
- [14] MM Popovic and BN Grgur. *Synth Met* 2004;142(2):191- 195.
- [15] JI Martins, M Bazzouai, TC Reis, EA Bazzouai and LI Martins. *Synth Mat* 2002;129:221- 228.
- [16] M Bazzouai, LI Martins, EA Bazzouai and TI Martins. *Electrochem Acta* 2002;47:2953 - 2962.
- [17] SR Moraes, DH Vilca and AJ Motheo. *Prog Org Coat* 2003;48:28 - 33.
- [18] L Wang, P Brazis, M Rocci, CR Kannewurf and MG Kanatzidis. *Chem Mater* 1998;10:3298 - 3300.
- [19] S Yashimoto, F Ohasni, Y Ohnishi and T Nonmai. *Synth Met* 2004;145:265 - 270.
- [20] S Yashimoto, F Ohasni and T Kameyama. *Macromol Rapid Commun* 2004;25:1687 - 1697.
- [21] AG Mac Diarmid and AJ Epstein. *Faraday Discuss Chem Soc* 1989;88:317 - 324.
- [22] S Yashimoto, F Ohasni, Y Ohnishi and T Nonmai. *Chem Commun* 2004;50:1924 - 1925.
- [23] Q Wu, Z Xue, Z Qi and F Wang. *Polymer* 2000;41:2029 - 2032.
- [24] E Akbarinezhad, M Ebrahimi, F Sharif, MM Atter and HR Faridi. *Prog Org Coat* 2011;70:39-44.
- [25] SK Mondal, K Rajendra Prasad and N Munichandraiah. *Synth Met* 2005;148:275- 286 .
- [26] P Pawar, AB Gaikwad and PP Patol. *Electrochimica Acta* 2007;52:5958-5967.
- [27] SS Deng and L Guang. *J Adv Mater Res* 2012;476-478:809-813.